nature photonics

SUPPLEMENTARY INFORMATION

DOI: 10.1038/NPHOTON.2013.192

Supplementary information: Linear Momentum Increase and Negative Optical Forces at Dielectric Interface

Veerachart Kajorndejnukul[1], Weiqiang Ding[2], Sergey Sukhov[1], Cheng-Wei Qiu[2], Aristide Dogariu[1]

[1]*CREOL, The College of Optics and Photonics University of Central Florida, 4000 Central Florida Boulevard Orlando, Florida 32816, USA*

[2]*Department of Electrical and Computer Engineering, National University of Singapore, 4 Engineering Drive 3, Singapore 117576, Singapore*

1 The scattering force calculation and momentum of electromagnetic wave in medium

In the main text, we calculate the optical force using a ray tracing method (RTM). In the RTM calculation, the incident light beam is regarded as a bundle of N optical rays, (N was of the order of several thousands in our calculations), each ray carrying m photons with a momentum of $m\boldsymbol{p}$ and energy of mE_0. Here $\boldsymbol{p}$ and $E_0 = \hbar\omega$ are the momentum and energy carried by a photon. Then, the momentum changes for each ray Δp can be calculated by a ray tracing method based on the Fresnel reflection and refraction formulations with the consideration of polarization, refractive indices, and incident angle. A ray experiences multiple reflections and refractions when it is incident onto the scatterer. During this process, the momentum change of the ray may be determined by accounting for the direction and strength of the transmissions and reflections:

$$\begin{aligned}\Delta\mathbf{P}_{\text{ray}} &= \Delta\mathbf{P}_{\text{ray},1} + \Delta\mathbf{P}_{\text{ray},2} + \cdots \\ &= P_0(R_1\mathbf{A}_{1r} + T_1T_2\mathbf{A}_{2t} + T_1R_2\mathbf{A}_{2r} - \mathbf{A}_{1i} + \cdots)\end{aligned}$$

Here P_0 is the amplitude of the momentum of the incident ray, $\mathbf{A}_{ni,nt,nr}$ are the directional vectors along the incident, transmission, and reflection rays for the n-th refraction, $T_{1,2}$ and $R_{1,2}$ are energy transmission and reflection coefficients determined by the Fresnel formulas. For a given incident vector $\mathbf{A}_i$, the transmission and reflection vectors are determined by the following vector form[1]

$$\begin{aligned}\mathbf{A}_t &= \mathbf{A}_i + Q\cdot\mathbf{n} \\ \mathbf{A}_r &= \mathbf{A}_i - 2\mathbf{n}(\mathbf{n}\cdot\mathbf{A}_i)\end{aligned}$$

DOI: 10.1038/NPHOTON.2013.192

Here $\mathbf{n}$ is the outward normal unit vector, Q is a function of incident angle φ $Q=\sqrt{n''^2-n'^2+n'^2\cos^2\varphi}-n'\cos\varphi$, n' and n'' denote the refractive indices of incident and transmission sides, respectively. In this representation Q assumes Minkowski mechanism for the change of photon momentum. Then we can calculate the total changes of the momentum of the incident light beam as $\Delta\mathbf{P}=\sum\Delta\mathbf{P}_{ray}$ where only the rays hitting the scatterer are involved.

2 Normal force on a surface bound particles

In the main text we considered only the tangential component of the optical force. In this section, we add to this discussion and present the features of the normal component of the force. Let us again consider a scatterer with refractive index of n_3 placed at the interface of two media with refractive indices n_1 and $n_2 > n_1$. The scatterer is illuminated by a beam of light (plane wave) such that some of the incident and the scattered rays lie in different media (see Figure 1 in the main text). According to Minkowski's approach, when going from medium 1 to 2 the momentum increases and, consequently, the scattering force may become negative such that the total momentum is conserved. It was shown in the main text that the tangential component of the force becomes negative for a variety of shapes and incidence angles. In Figure 1S we present similar calculations made for the normal component of the force F_z. As one can see, the normal component of the force is also negative for a large range of parameters. Thus, in our treatment one can conclude that not only a *component* of the force is attractive but, in general, the entire optical force is. However, this normal force cannot overcome surface tension forces (see Section 5 below) and is not observable in our experiment.

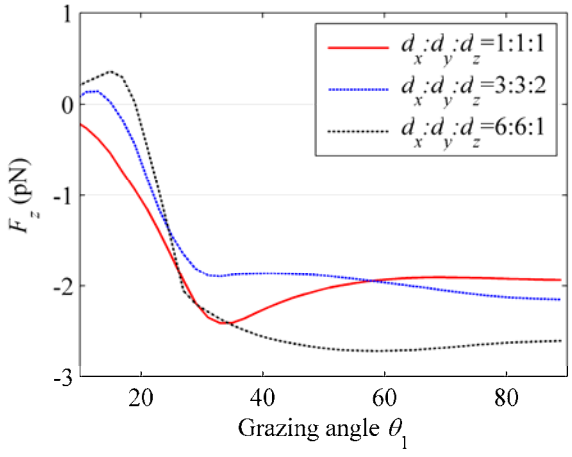

Figure 1S. The normal component of optical force exerted on spheroids with different main axes d_x, d_y and d_z, but having the same cross-section area along the interface ($d_x \cdot d_y = \text{const}$, $d_x = d_y = 10\mu m$). The forces are calculated with a ray tracing technique for spheroids with refractive index $n_3 = 1.42$ floating at the air-water interface and being illuminated by a p-polarized plane wave with the irradiance of $10\mu\text{W}/\mu\text{m}^2$.

3 Additional experiments on different liquid system

Additionally to dodecane, we performed experiments with another type of oil. The similar procedure as described in Materials and Methods section of the main text was followed to form micron-sized oil droplets on the surface of water. Fused silica index-matching oil (refractive index $n = 1.4587$, Cargille Laboratories Inc.) was dissolved in pentane in a proportion 1:3000 by volume. Tiny amount of the solution (~0.2 μL) were gently released from 10μL syringe onto the surface of water. After the rapid evaporation of pentane, the oil droplets of index matching liquid were spontaneously formed on the water surface. As a result, oil drops with diameters ranging from 8 μm to 30 μm were obtained (see Media File 2). The floating oil droplets were illuminated by p- polarized monochromatic (wavelength 532nm) 2W beam loosely focused into ≈ 300μm spot. Particles inside illumination spot demonstrated clear movement against the direction of incident beam. No apparent optically induced motion was detected for the case of s-polarized light that shows clear dependence of the effect on the properties of incident light and can be used to switch on and off the discussed effect.

4 The shape of floating oil drops

The shape of the liquid drops on a liquid-air interface is defined by characteristic capillary lengths[2]:

$$\kappa_w^{-1} = \sqrt{\frac{\gamma_w}{\rho_w g}}, \quad \kappa_o^{-1} = \sqrt{\frac{\gamma_o}{\rho_o g}}, \quad \kappa_{wo}^{-1} = \sqrt{\frac{\gamma_{wo}}{(\rho_w - \rho_o) g}}, \qquad (1S)$$

where subscript "w" stands for "water" and "o" stands for "oil"; g is the gravitational acceleration, $\rho_{w,o}$ are densities of the water and oil, and $\gamma_{w,o}$ are the surface tension coefficients. Surface tension coefficients and density of dodecane and water are known[3,4]: $\gamma_{wo} \approx 52$ mN/m, $\gamma_o \approx 25$ mN/m, $\gamma_w \approx 72$ mN/m, $\rho_0 = 0.7808$ g/cm^3. Substituting these parameters into Eqs.(1S), one can find that in the case of oil used in our experiments, all characteristic lengths are of the order of 1mm that is much larger than the size of used oil drops ~ 10μm. In this case the effects of gravity are negligible and droplet can be considered to be made from two spherical caps (see Figure 2S). Also, a droplet is located on a flat undisturbed water surface. Neumann's vector relation[2,3] $\boldsymbol{\gamma}_w + \boldsymbol{\gamma}_o + \boldsymbol{\gamma}_{wo} = 0$ specifies the angles determining the shape of a liquid drop (Figure 2S): $\varphi_1 = 31.4°$, $\varphi_2 = 14.5°$.

During the movement of particle, drag forces arise that can potentially change the shape of oil drop. However, the magnitude of these forces ($\sim \eta_o v$, where η_o is the viscosity of dodecane and $v \approx 3$μm/s is the typical velocity of oil drops in our experiments) is much smaller than surface tension forces ($\eta_o v << \gamma_o$) so that the possible shape changes are negligible.

DOI: 10.1038/NPHOTON.2013.192

In overdamped regime of particles movement, the magnitude of the tangential optical forces is equal to the drag forces. Thus, the deformation produced by tangential optical forces is also insignificant. One should also consider possible changes in the shape of the drop due to the influence of the optical forces normal to the surface. Figure 3S shows theoretical estimation for the normal component of the optical force acting on droplets. One can see that for the grazing angle 25° used in experiment the force is $F_z^p / I \approx -38\text{pN}/(\text{mW}/\mu\text{m}^2)$ for p-polarization and $F_z^s / I \approx -23\text{pN}/(\text{mW}/\mu\text{m}^2)$ for s-polarized incident wave that is of the same order of magnitude as the tangential force. Thus, the normal component of the force is not expected to induce any modifications in the oil drop shape.

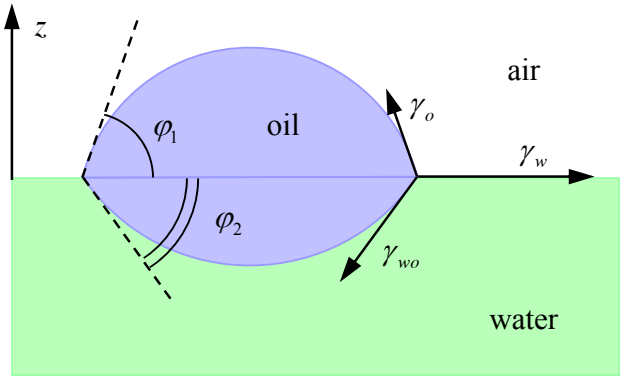

Figure 2S. Circular lens of oil drop resting on a liquid surface. The angles φ_1, φ_2 determining the shape of the drop are defined by surface tension coefficients γ_o, γ_w, γ_{wo}.

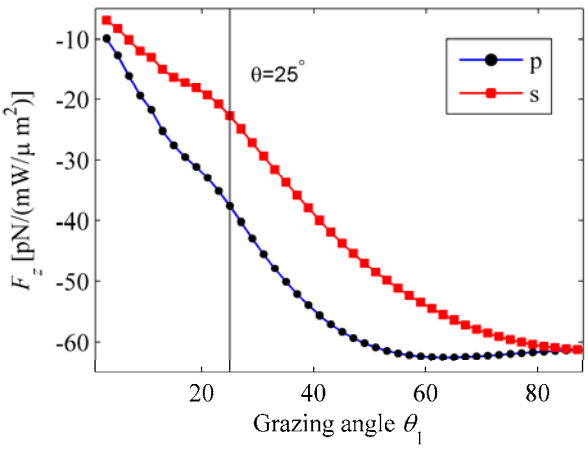

Figure 3S. Optical force acting along the normal to the surface on a lens-like oil drop $10\mu\text{m}$ in diameter as a function of grazing angle θ_1 for s- and p- polarized incident waves as indicated.

5 Drag force on floating liquid drops

Let us consider the tangential motion of the scatterer along the water-air interface. Aside from the optical scattering force, a resistance force will appear as soon as the scatterer begins to move. In laminar regime, the drag force is[5]

$$F_d = -b \cdot v ,$$

where v is the velocity of the scatterer relative to water, and b is the drag coefficient, which is determined by the properties of both the liquid (water) and the scatterer.

To determine the drag coefficient b for the dodecane oil droplets used in experiment, we observed the Brownian motion of these particles. The trajectories of the particles were then reconstructed using a particle tracking technique. After all the trajectories were recorded, the mean square displacement of the particles was calculated as a function of time (Figure 4S). To eliminate the influence of the collective motion of the particles, a relative mean square displacement of pairs of particles was used[6]:

$$MSD_{rel} = \left\langle \Delta r_{rel}^2(\tau) \right\rangle = \left\langle \left(\Delta \mathbf{r}_{ij}(t+\tau) - \Delta \mathbf{r}_{ij}(t) \right)^2 \right\rangle = 8D\tau ,$$

where $\Delta \mathbf{r}_{ij}$ is the vector difference between positions i-th and j-th particles, and D is the diffusion coefficient. In order to further eliminate the possible effects of nonuniformity of macroscopic flows, only particle pairs floating within $\sim 300\,\mu\text{m}$ of each other were considered. Moreover, to avoid the influence of possible hydrodynamic interactions, we tracked only those particles that did not have any neighbors within seven diameters ($\approx 70\,\mu\text{m}$).

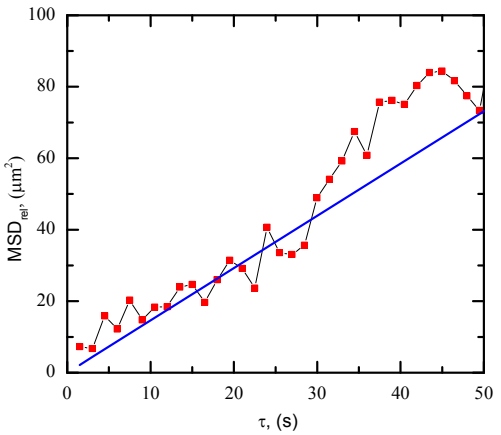

Figure 4S. Relative mean square displacement MSD_{rel} for dodecane oil droplets with diameters $10.6 \pm 0.4 \mu m$ at the water/air interface. Symbols show experimental data, straight line shows weighed least squares fit to the experimental data.

The diffusion coefficient for floating dodecane droplets was found to be $D = 0.18 \pm 0.01 \mu\text{m}^2/\text{s}$. With that, the drag coefficient of the dodecane drops is found to be $b = k_B T / D = (2.3 \pm 0.1) \cdot 10^{-8}\ \text{N} \cdot \text{s/m}$. This value of the drag coefficient is approximately 4 times smaller than that for a solid sphere of the same size in the bulk of the liquid.

DOI: 10.1038/NPHOTON.2013.192

6 The effect of convective flows

When illuminated by incident light, the small floating lenses used in our experiment focus a light inside the water (see, for example, Figure 3a in the main text). The increased light intensity in this focus can act as a local heat source because of residual absorption in the water (water absorption coefficient is $3.5 \cdot 10^{-4}\,\mathrm{cm}^{-1}$ for illumination wavelength 532nm). This heated water can create convective flows that can influence the droplets motion. The purpose of the section is to estimate the magnitude of those flows on the air-water surface.

The location of the focus inside the water can be estimated from the lens theory[7]. For the parameters described in Section 4, the focus is located 26.5μm below the surface of the water and 44.5μm away from the center of the lens in horizontal direction. For simplicity, we approximated the field distribution behind the lens in the water as a Gaussian beam. The beam created by a 10μm lenslet would have a waist of 1.9μm. Note that this approximation overestimates thermal effects as the real focus region is heavily distorted by aberrations due to highly non-paraxial illumination.

The coupled thermal and hydrodynamic system was modeled with a commercial finite elements computer program (Comsol Multiphysics 3.5a). A large water volume (800μm×800μm×150μm) was simulated to eliminate boundary effects and the volume heat sources were defined by Gaussian beam mentioned above. Results of simulations are shown in Fig. 5S and, as can be seen, the typical magnitude of convection flows in the vicinity of a lenslet is of the order of pm/s that is significantly smaller than the velocities observed in the experiment (μm/s).

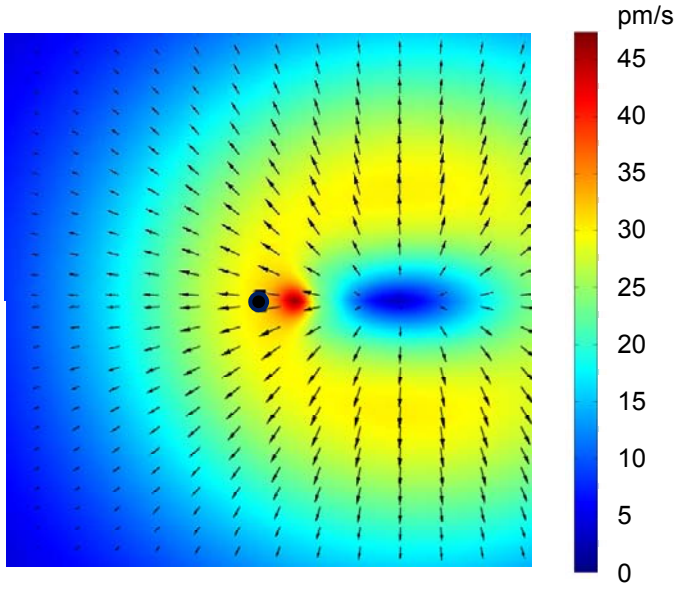

Figure 5S. The velocity of convection flows at the air-water interface. The color scale denotes the magnitude of the velocity while the arrows show the direction of local flows. The position of the 10μm lenslet is indicated by the small dot in the middle. The irradiance of the light at the surface is $35\mu\mathrm{W}/\mu\mathrm{m}^2$. The beam propagates from left to right and is incident on the water surface at a grazing angle 25°.

Media File 1 – The dynamics of dodecane droplets at the water/air interface under the illumination with p-polarized 1.2W Gaussian beam. The ellipsis shows the $1/e^2$ intensity outline of the beam. The arrow indicates the direction of the propagation of incident beam. The speed of the movie was increased 3X times.

Media File 2 - The dynamics of index matching oil ($n = 1.4587$) droplets at the water/air interface under the illumination with p-polarized 1.2W Gaussian beam. The ellipsis shows the $1/e^2$ intensity outline of the beam. The arrow indicates the direction of the propagation of incident beam. The speed of the movie was increased 9X times.

References

1. Tkaczyk, E. R. Vectorial laws of refraction and reflection using the cross product and dot product. *Opt. Lett.* **37**, 972-974 (2012).
2. de Gennes, P.-G., Brochard-Wart, F. & Quéré, D. *Capillarity and Wetting Phenomena: Drops, Bubbles, Pearls, Waves*. (Springer, Berlin, 2003).
3. Aveyard, R. & Clint, J. H. Liquid lenses at fluid/fluid interfaces, *J. Chem. Soc., Faraday Trans,* **93**, 1397-1403 (1997).
4. David, R., Dobson, S. M., Tavassoli, Z., Cabezas, M. G. & Neumann, A.W. Investigation of the Neumann triangle for dodecane liquid lenses on water, *Colloids and Surfaces A: Physicochem. Eng. Aspects* **333,** 12–18 (2009).
5. Batchelor, G. K. *An Introduction to Fluid Dynamics*. (Cambridge University Press, 1967).
6. Ortega, F., Ritacco, H. & Rubio, R. G. Interfacial microrheology: Particle tracking and related techniques. *Current Opinion in Colloid & Interface Science* **15,** 237–245 (2010).
7. Hecht, E. *Optics*. (Addison Wesley, Reading, MA, 2001).